AGU ADVANCING EARTH AND SPACE SCIENCE

JGR Space Physics

RESEARCH ARTICLE
10.1029/2020JA027995

Key Points:
- Interhemispheric conjugacy of throat aurora is examined by the associated geomagnetic responses under quiet solar wind conditions
- Concurrent onsets followed by poleward moving signature are evidence supporting throat aurora being caused by magnetopause reconnection
- *X* component increases observed after the concurrent onsets can be regarded as micropositive bays caused by a pair of field-aligned currents

Correspondence to:
D.-S. Han,
handesheng@tongji.edu.cn

Citation:
Feng, H.-T., Han, D.-S., Chen, X.-C., Liu, J.-J., & Xu, Z.-H. (2020). Interhemispheric conjugacy of concurrent onset and poleward traveling geomagnetic responses for throat aurora observed under quiet solar wind conditions. *Journal of Geophysical Research: Space Physics*, *125*, e2020JA027995. https://doi.org/10.1029/2020JA027995

Received 14 MAR 2020
Accepted 27 MAY 2020
Accepted article online 22 JUL 2020

Interhemispheric Conjugacy of Concurrent Onset and Poleward Traveling Geomagnetic Responses for Throat Aurora Observed Under Quiet Solar Wind Conditions

Hui-Ting Feng[1], De-Sheng Han[1], Xiang-Cai Chen[2], Jian-Jun Liu[2], and Zhong-Hua Xu[3]

[1]State Key Laboratory of Marine Geology, School of Ocean and Earth Science, Tongji University, Shanghai, China, [2]MNR Key Laboratory for Polar Science, Polar Research Institute of China, Shanghai, China, [3]Bradley Department of Electrical and Computer Engineering, Virginia Polytechnic Institute and State University, Blacksburg, VA, USA

Abstract Throat auroras frequently observed near local noon have been confirmed to correspond to magnetopause indentations, but the generation mechanisms for these indentations and the detailed properties of throat aurora are both not fully understood. Using all-sky camera and magnetometer observations, we reported some new observational features of throat aurora as follows. (1) Throat auroras can occur under stable solar wind conditions and cause clear geomagnetic responses. (2) These geomagnetic responses can be simultaneously observed at conjugate geomagnetic meridian chains in the Northern and Southern Hemispheres. (3) The initial geomagnetic responses of throat aurora show concurrent onsets that were observed at all stations along the meridians. (4) Immediately after the concurrent onsets, poleward moving signatures and micropositive bays were observed in the *X* components at higher- and lower-latitude stations, respectively. We argue that these observations provide evidence for throat aurora being generated by low-latitude magnetopause reconnection. We suggest that the concurrent onsets reflect the instantaneous responses of the reconnection signal arriving at the ionosphere, the followed poleward moving signatures reflect the antisunward dragging of the footprint of newly opened field lines, and the micropositive bays may result from a pair of field-aligned currents generated during the reconnection. This study may shed new light on the geomagnetic transients observed at cusp latitude near magnetic local noon.

1. Introduction

In the cusp region, auroras can be observed by optical instruments in the red (λ ~ 630.0 nm) and the green (λ ~ 557.7 nm) lines but are predominant in the red line (e.g., Sandholt & Newell, 1992). In this region, the equatorward edge of the red line aurora has been generally accepted as the open-closed field line boundary (Chen et al., 2017; Lockwood, 1997; Moen et al., 1996). For a long time, this boundary has been regarded as a roughly smooth boundary and been supposed to correspond to the roughly smooth magnetopause near the subsolar point. Recently, it has been noticed that the equatorward edge of the red line aurora near local noon is not a smooth boundary at all but is often attached by some north-south aligned auroral structures that have been named "throat aurora" (Han et al., 2015). Using coordinated ground and satellite observations, Han et al. (2016, 2018) presented evidence that throat auroras are the ionospheric signature of magnetopause indentations. In addition, because the throat aurora has rather high occurrence rate and has various spatial scales (Han et al., 2017), it has been inferred that the subsolar magnetopause should have some corresponding indentations in different sizes. How these indentations are generated is certainly important for understanding the solar wind-magnetosphere-ionosphere coupling, but it is not clear yet.

The detailed properties of throat aurora are of great significance in investigating how these magnetopause indentations are generated, but they have not been fully understood. Up to the present, it has been revealed that (1) throat auroras are caused by precipitation of magnetosheath particles that are on the open filed lines (Han et al., 2016), (2) throat auroras are often observed to appear from a background of diffuse aurora that is on the closed field lines (Han et al., 2015, 2016), (3) occurrence of throat aurora shows little dependence on the interplanetary magnetic field (IMF) Bz component but shows clear dependence on the IMF cone angle (Han et al., 2017), (4) throat auroras correspond to magnetopause indentations (Han et al., 2016, 2018) and

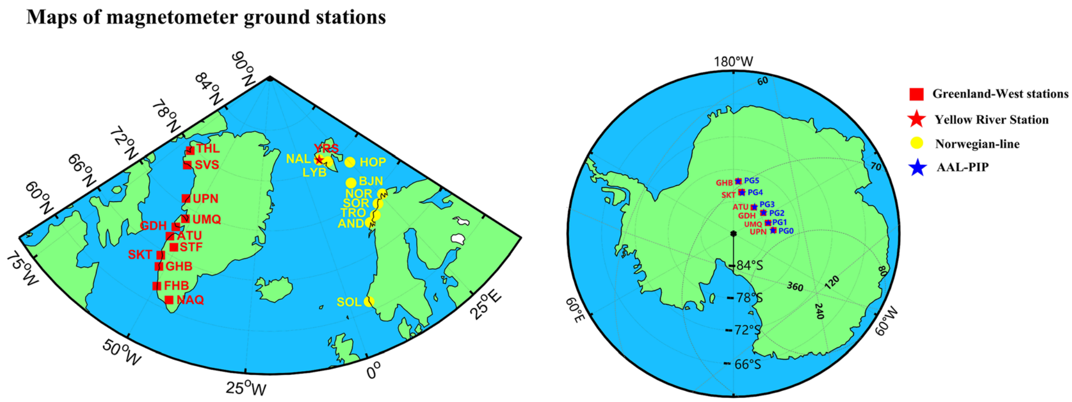

Figure 1. The location of ground stations used in the study. The left and right panels indicate the stations in the Northern and Southern Hemispheres, respectively. Greenland-West stations and Norwegian line stations in the Northern Hemisphere are marked with red squares and yellow dots, respectively. Location of YRS is indicated by red pentagram, where is at the same location as NAL station. The right panel indicates the locations of AAL-PIP that are marked with blue pentagram. The conjugate Greenland-West stations are marked with red squares.

the depth of the magnetopause indentation can be >3.0 Re (Earth Radius) as inferred from the throat auroras observed on the ground (Han et al., 2017), and (5) throat auroras show clear reconnection signatures in the EISCAT radar observations (Han et al., 2019). Based on the above observations, Han (2019) suggested that throat auroras are likely caused by a particular magnetopause reconnection that can deeply develop inward the magnetosphere at a much localized sector. For a magnetopause reconnection occurred between the two cusps, the interhemispheric conjugacy, that is, similar responses observed at the geomagnetically conjugate stations in the Northern and Southern Hemispheres, is expected. For the first time, this study will investigate the interhemispheric conjugacy for throat aurora by using geomagnetic observations.

In addition, the geomagnetic responses associated with throat aurora show similar waveform as the geomagnetic transients, such as magnetic impulse events (MIEs) (e.g., Lanzerotti et al., 1990), traveling convection vortices (TCVs) (e.g., Friis-Christensen et al., 1988), and impulsive ultralow frequency (ULF) waves (e.g., Olson, 1986), which have been extensively studied. This study will show that the geomagnetic responses associated with throat aurora have some new properties that have not been reported in the previous studies on geomagnetic transients. With the aid of the two-dimensional information provided by aurora, this study may shed new light on the geomagnetic transients observed near magnetic local noon.

2. Data and the Event

The IMF and solar wind data used in this study are extracted from the National Aeronautics and Space Administration/Goddard Space Flight Center (NASA/GSFC)'s OMNI data set through OMNIWeb. The optical observations are obtained from Yellow River Station (YRS) at Ny-Ålesund, Svalbard (geomagnetic latitude 76.24°N). The optical system at YRS consists of three identical all-sky imagers equipped with band-pass filters at 557.7 (green line), 630.0 (red line), and 427.8 nm, respectively, and has been continuously run since 2003. Only the red line observations are used in this paper.

Geomagnetic field variations observed by fluxgate magnetometers at geomagnetically conjugate stations in the Northern and Southern Hemispheres are used to investigate the conjugate properties of throat aurora. Figure 1 shows the location of the stations used in this study. Table 1 gives the detailed information about the stations. In the Northern Hemisphere, geomagnetic data along two meridian lines of the geomagnetic longitude ~110.0°E (i.e., Norwegian line) and ~40.0°E (i.e., Greenland-West line) were obtained from Tromsø Geophysical Observatory. The geomagnetic station of NAL is at the same location as YRS, where the auroral observations were made. In the Southern Hemisphere, Autonomous Adaptive Low-Power Instrument Platform (AAL-PIP) line was designed and established by the University of Michigan Space Physics Research Laboratory in the Antarctica. The AAL-PIP line consists of six stations named PG0, PG1, PG2, PG3, PG4, and PG5, which are along the geomagnetic longitude ~40.0°E and are ranging from

Table 1
List of Magnetometer Ground Stations in the Study

Station	Station code	Geographic latitude	Geographic longitude	Geomagnetic latitude	Geomagnetic longitude	MLT of UT 0000
			Greenland-West stations			
Thule	THL	77.47	290.77	84.94	29.36	21.41
Savissivik	SVS	76.02	294.90	83.20	32.93	21.64
Upernavik	UPN	72.78	303.85	79.07	40.16	22.13
Umanaq	UMQ	70.68	307.87	76.50	42.48	22.28
Godhavn	GDH	69.25	306.47	75.38	39.18	22.06
Attu	ATU	67.93	306.43	74.13	37.93	21.98
Kangerlussuaq	STF	67.02	309.28	72.76	40.64	22.16
Sukkertoppen	SKT	65.42	307.10	71.58	36.91	21.91
Godthaab	GHB	64.17	308.27	70.14	37.54	21.95
Frederikshaab	FHB	62.00	310.32	67.58	38.73	22.03
Narsarsuaq	NAQ	61.16	314.56	65.90	42.93	22.31
			AAL-PIP stations			
Antarctic	PG0	−83.67	88.68	−78.31	38.09	21.99
	PG1	−84.50	77.20	−76.91	37.18	21.93
	PG2	−84.42	57.96	−75.17	38.83	22.04
	PG3	−84.81	37.63	−73.42	36.43	21.88
	PG4	−83.34	12.25	−70.66	35.99	21.85
	PG5	−81.96	5.71	−69.25	36.76	21.80
			Norwegian line stations			
Ny Ålesund	NAL	78.92	11.93	76.25	110.21	2.72
(Yellow River Station)	(YRS)					
Longyearbyen	LYB	78.20	15.83	75.31	111.20	3.09
Hopen	HOP	76.51	25.01	73.15	114.57	2.61
Bjørnøya	BJN	74.50	19.00	71.53	107.51	2.72
Nordkapp	NOR	71.09	25.79	67.79	109.06	2.72
Sørøya	SOR	70.54	22.22	67.41	105.83	2.50
Tromsø	TRO	69.66	18.94	66.70	102.56	2.29
Andenes	AND	69.30	16.03	66.50	100.02	2.12
Solund	SOL	61.08	4.84	58.62	86.00	1.18

~70.0°S to ~80.0°S in the geomagnetic latitude. More importantly, the AAL-PIP stations are geomagnetically conjugate to some stations in the Greenland-West line. In Figure 1, the Greenland-West stations and the Norwegian line stations are indicated by red squares and yellow dots, respectively. The AAL-PIP stations, that is, PG1-PG5, are indicated in blue pentagons. The Greenland-West stations that are approximately conjugate to PG1-PG5 (Xu et al., 2019) are also plotted in the Antarctic map.

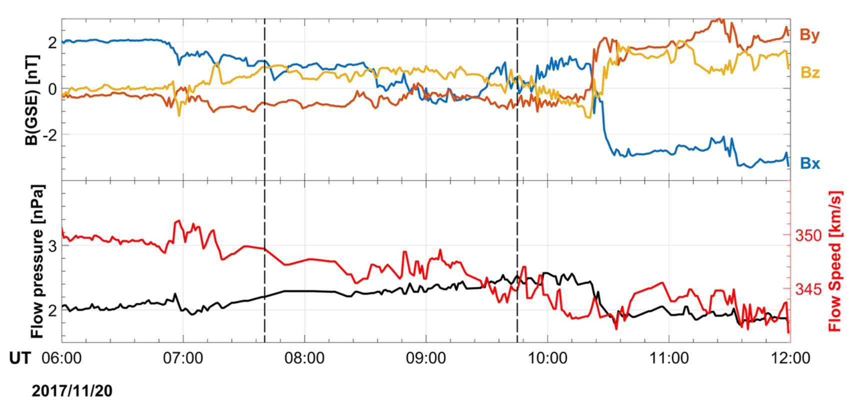

Figure 2. The OMNI data for the event observed on 20 November 2017. The upper panel shows the IMF Bx, By, and Bz. The bottom panel shows the solar wind speed and dynamic pressure. The two vertical dash lines indicate the time period, during which the throat auroras were observed.

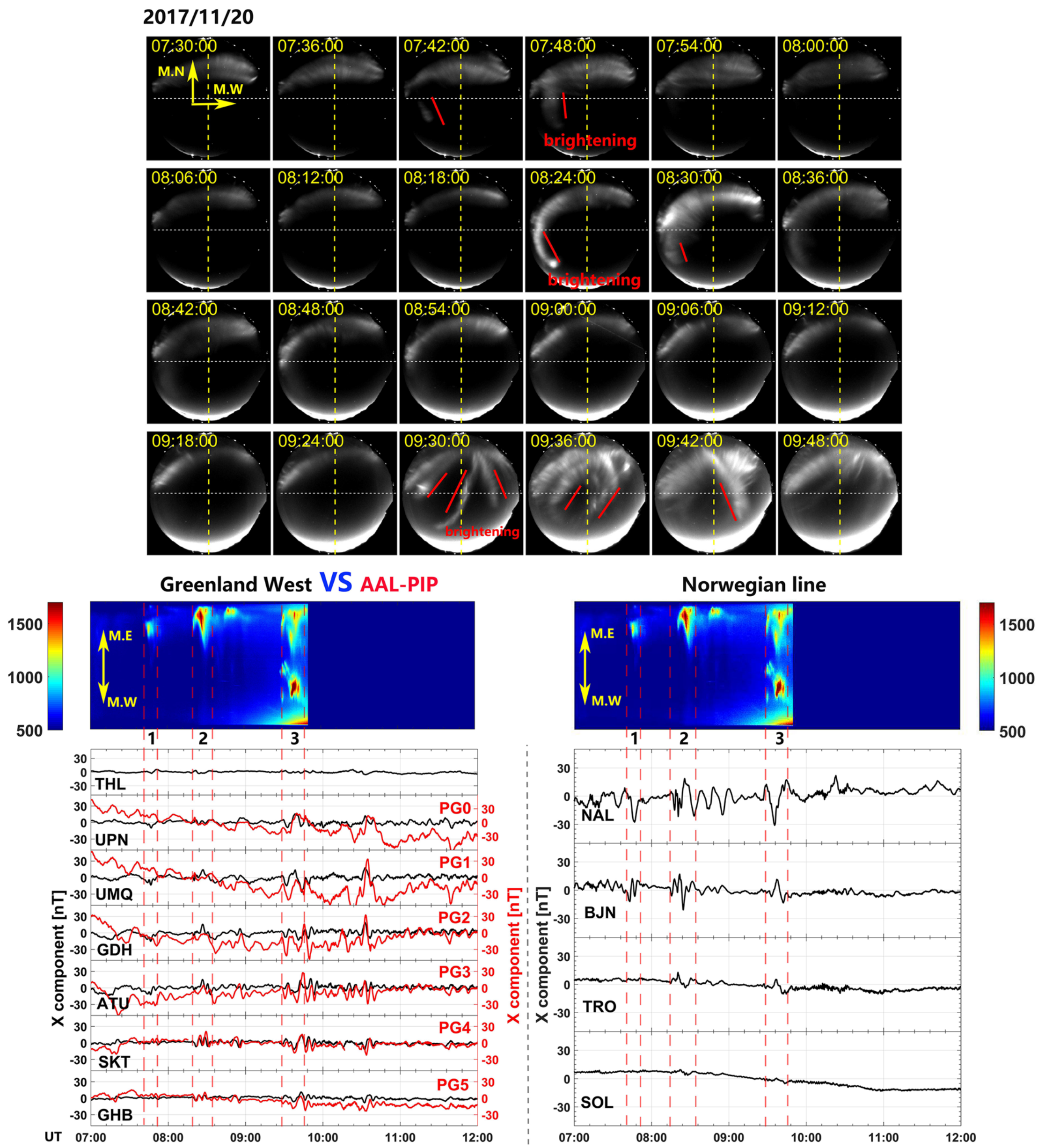

Figure 3. Throat aurora events and the geomagnetic observations on 20 November 2017. The top panels show the auroral images in red line (λ ~ 630.0 nm) from 07:30 to ~09:50 UT with 6-min interval. The magnetic north and magnetic west are indicated as "M.N" and "M.W" in the first auroral image. Some red bars plotted in the image are used to indicate the throat auroras. The middle panels show the E-W keogram that is obtained by taken a slice of data along the east-west direction from each auroral image and reorganizing the data by time. The bottom left and bottom right panels show the *X* components observed at Greenland-West versus AAL-PIP stations and at Norwegian line stations, respectively. The vertical dash red lines indicate three throat aurora events that are respectively labeled with "1," "2," and "3."

The main purpose of this work is to check the interhemispheric conjugacy of throat aurora. In order to get the definite responses of throat aurora, it is better to select isolated throat auroras occurred during quiet geomagnetic condition. Under such conditions, both the auroral and geomagnetic variations are easy to define. Based on these criteria, an ideal event on 20 November 2017 was selected.

3. Observations

Figure 2 shows the OMNI data for the event observed on 20 November 2017. The top and bottom panels show the IMF Bx, By, and Bz components in the geocentric solar ecliptic (GSE) coordinate, and the solar wind bulk speed and dynamic pressure, respectively. The two vertical dash lines indicate the time period when three isolated throat auroras were observed. We see that the solar wind conditions during this time period are relatively stable and quiet. The IMF Bz is positive and is weak, that is, ~1.0 nT. The IMF By is in weak negative.

Figure 3 shows the auroral and geomagnetic field observations on 20 November 2017. The upper panels show the auroral images observed at YRS with 6-min interval. The bottom left panel shows the observations from some stations along the Greenland-West line in the Northern Hemisphere and along the AAL-PIP line in the Southern Hemisphere. The bottom right panel shows some observations along the Norwegian line. The auroral E-W keograms are plotted above each column of the geomagnetic observation in order to make a comparison between the aurora and geomagnetic variations. The E-W keogram is obtained by taking a slice of data along the east-west direction from each auroral image (as indicated by the white dash lines on each image shown in Figure 3) and reorganizing the data by time. There is no auroral observation after 09:50 UT. The geomagnetic variations associated with the throat auroras are summarized as follows.

a. *Quasiperiodic occurrence and interhemispheric conjugacy of throat aurora*. In Figure 3, three isolated throat aurora events were observed at ~07:41–07:51, ~08:19–08:34, and ~09:28–09:45 UT, respectively. For these events, the throat aurora brightenings are marked out by the red bar. From E-W keogram, we estimate the duration time of the three events is ~10, 15, and 17 min, respectively. Here we note that these throat auroras appear to occur with a somewhat periodic or quasiperiodic nature when the solar wind conditions, as shown in Figure 2, were stable, which is a new property of throat aurora that has not been discussed before.

Corresponding to these throat auroras, clear geomagnetic variations were observed as indicated between the dashed lines labeled with “1,” “2,” and “3.” When the three throat auroras were observed, the high-latitude Norwegian line stations (e.g., NAL, LYB) and auroral station (i.e., YRS) were at ~10:40, ~11:20, and ~12:20 MLT, respectively, while the high-latitude Greenland-West stations were approximately at ~06:30, ~07:10, and ~08:10 MLT, respectively.

First, we check the geomagnetic responses observed in the Northern Hemisphere (shown in black curves). For Events “1” and “2,” the throat auroras appeared at the east edge of the field of view of all-sky camera, which mean that the throat aurora locations were closer to the Norwegian line stations but were far away from the Greenland-West stations. This explains why the geomagnetic responses observed at Norwegian line stations associated with these two events are much clearer than those observed at Greenland-West stations. For Event “3,” the throat aurora appeared at slightly west of the zenith and both the Norwegian line and Greenland-West stations observed clear geomagnetic responses. If we focus on the third event that have the clearest geomagnetic responses, the waveforms observed at PG1/UMQ are more like MIEs (e.g., Lanzerotti et al., 1990), but those observed at lower latitude at PG3/ATU and PG4/SKT are more like impulsive ULF waves. For all the three events, the geomagnetic variations observed at THL in the polar cap were very weak.

The bottom left panel of Figure 3 shows that similar variations were observed at the conjugate station pairs between the Northern and Southern Hemispheres. We therefore conclude that conjugate properties of throat aurora were identified in this case.

b. *The concurrent onsets for geomagnetic responses*. In Figure 3, Event “3” has the clearest geomagnetic responses observed at all stations. In order to investigate the details of the geomagnetic variations associated with the throat aurora, the observations for Event “3” are replotted in Figure 4 by adding plots from more stations.

In Figure 4, the E-W keograms and the geomagnetic observations from 09:10 to 09:50 UT observed at Greenland-West versus AAL-PIP and Norwegian line are shown in top left and top right, respectively. The geomagnetic plots from bottom to top are organized by increasing the geomagnetic latitude of the station. Some example auroral images observed during this time period are shown in the bottom. We focus on examining two concurrent onsets observed at ~09:28:30 and ~09:36:30 UT, respectively.

At ~09:28:30 UT, as indicated by the red vertical lines, the observational results can be summarized as follows. (1) A variation onset was simultaneously observed at almost all stations in the Northern

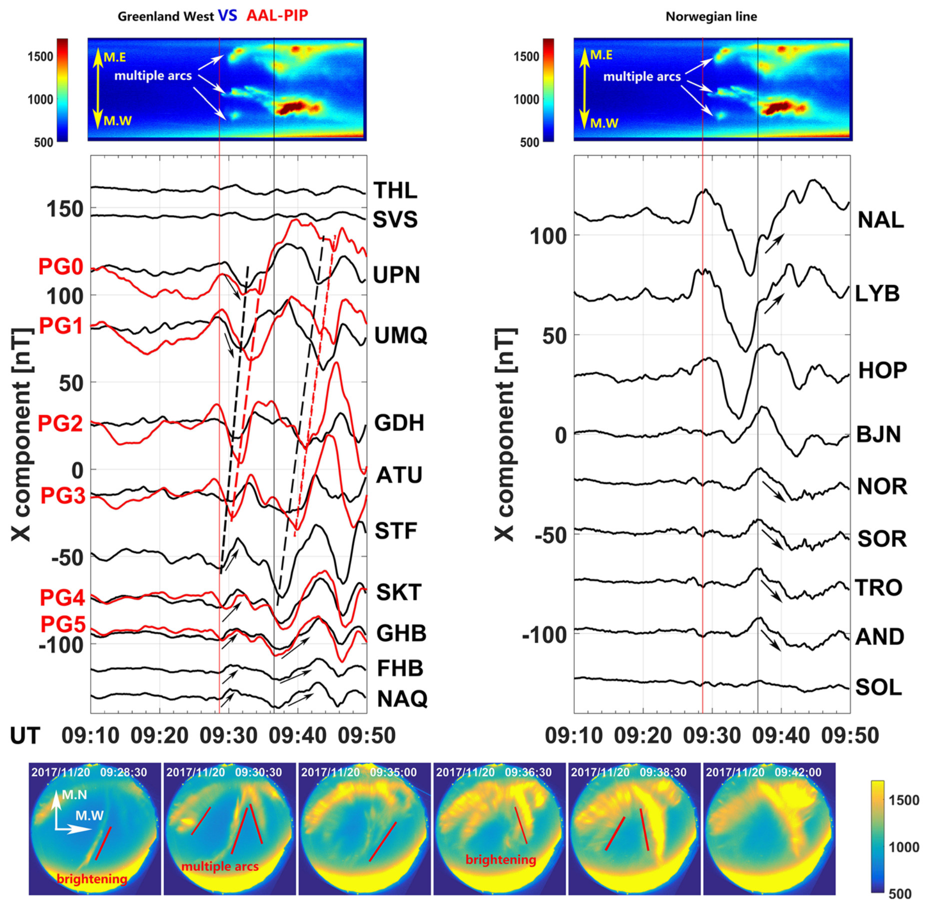

Figure 4. Detailed auroral and geomagnetic observations associated with the throat aurora observed at ~09:28–09:45, that is, Event "3" as shown in Figure 3. The top panels show E-W keogram, from which multiple arcs can be seen. The middle panels show the *X* component observed at Greenland-West versus AAL-PIP stations (left) and at Norwegian line stations (right). The plots from bottom to upper are organized by increasing the geomagnetic latitude of the station. Two vertical lines in red and black indicate the concurrent onsets observed at ~09:28:30 and ~09:36:30 UT, respectively. The black and red dash lines show poleward moving signatures observed in the Northern and Southern Hemisphere, respectively. In the bottom, some example auroral images observed during this time period are shown.

Hemisphere. (2) After the onset, the variations observed along the Greenland-West line show increase and decrease at lower-latitude (e.g., NAQ, FHB, GHB, and SKT) and higher-latitude stations (e.g., UPN, UMQ, and GDH), respectively, while the variations observed at STF and ATU seem like in the transitional stage. (3) This onset was associate with a throat auroral brightening that can be seen from the E-W keogram, as well as from the example auroral images.

At ~09:36:30 UT, as indicated by the black vertical lines, we see that a concurrent onset was observed at all stations too. Along the Greenland-West line, the variations observed at the lower- and higher-latitude stations after the onsets showed increases and decreases, respectively. The lower- and higher-latitude Norwegian line stations observed decreases and increases, respectively. This onset was also associated with a throat auroral brightening, as seen from the E-W keogram.

In a brief summary, we observed two onsets of geomagnetic variations that were concurrent at most of the stations. The two onsets were associated with two throat auroral brightenings. The variations observed after the onsets showed antiphase between lower- and higher-latitude stations along the same meridian.

In Figure 3, Event "2" observed at ~08:19–08:34 UT also show clear geomagnetic responses. In order to check if there also exists a concurrent onset for Event "2," we zoom in the variations for Event "2" and show the results in Figure 5 in the same format as Figure 4. We found that, at least, a geomagnetic variation onset

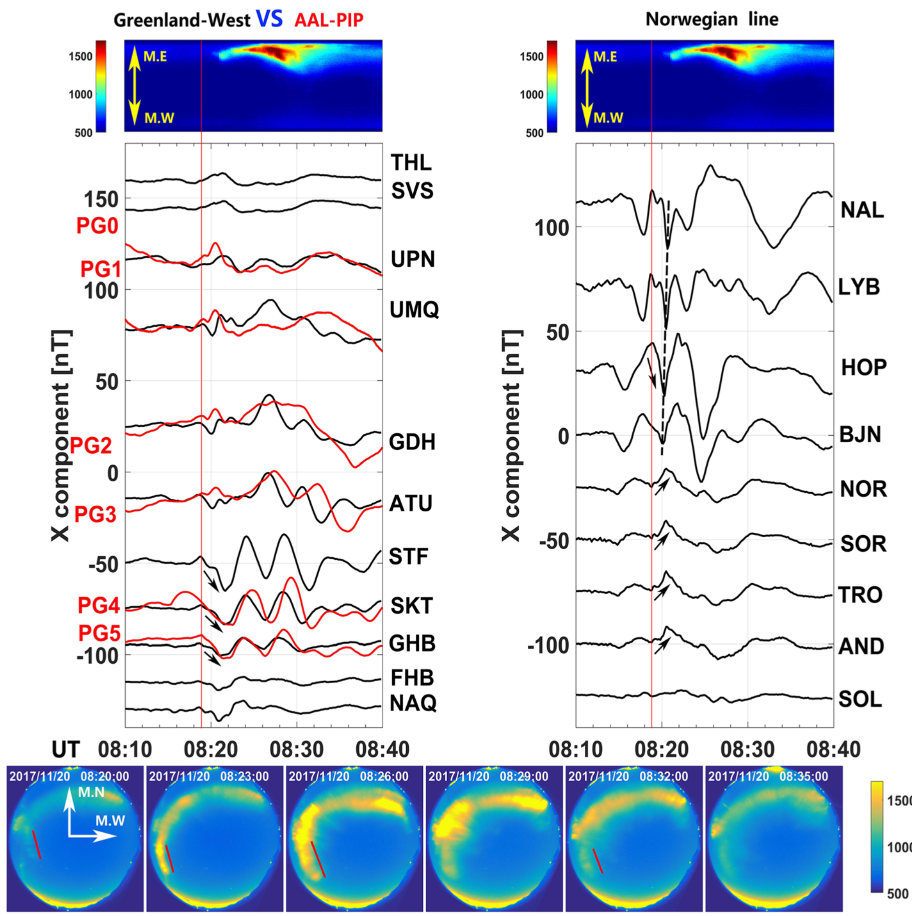

Figure 5. Detailed auroral and geomagnetic observations associated with the throat aurora observed at ~08:19–08:34, that is, Event "2" as shown in Figure 3. The format is the same as Figure 4.

at ~08:19:00 UT can be identified from all of the observations as indicated by the red vertical lines. The variations observed at lower- and higher-latitude stations along the Norwegian line show increases and decreases, respectively. This onset is also associated with a throat auroral brightening. All of these properties are consistent with the results shown in Figure 4.

The geomagnetic variations of Event "1," as shown in Figure 3, are not as clear as those of Events "2" and "3." We were not able to identify a clear concurrent onset for Event "1."

c. *The poleward moving signature and micropositive bays observed immediately after the concurrent onsets*. In Figure 4, as indicated by the oblique black and red dashed lines after the concurrent onset at ~09:28:30 UT, the negative peaks observed at higher-latitude stations along Greenland-West line in the Northern Hemisphere (black curves) and along the AAL-PIP line in the Southern Hemisphere (red curves) both show clear poleward moving signatures. The observations at lower-latitude stations, such as SKT, FHB, NHB, and NAQ, show similar increases. Here we call these increases micropositive bays, because we suggest that they reflect the similar physical processes as the midlatitude positive bays produced by the substorm current wedge on the nightside (McPherron et al., 1973) but with shorter time duration. After 09:36:30 UT, as indicated by the oblique dashed lines, similar poleward moving signatures were observed both in the Greenland-West and AAL-PIP observations too.

In Figure 5, after the concurrent onset at ~08:19:00 UT, a clear poleward moving signature can be seen at the higher-latitude stations along the Norwegian line as indicated by the black dashed line. At the same time, the lower-latitude stations observed micropositive bays, that is, *X* component increases.

In a brief summary, we find that a poleward moving negative peak can be often identified from the higher-latitude observations immediately after the concurrent onsets along a meridian. At the same time, we observed *X* component increases at lower-latitude stations after the onsets, which are named micropositive bays.

4. Summary and Discussion

This work aims to investigate the interhemispheric conjugate property for throat aurora. We selected a particular case of isolated throat auroras so that we can clearly identify the relevant effects. We observed three isolated throat auroras under stable and quiet solar wind conditions. These throat auroras are associated with clear geomagnetic responses, which are simultaneously observed at the conjugate stations from the Northern and Southern Hemispheres. Associated with the occurrence of throat aurora, concurrent onsets of geomagnetic variations are identified at all stations from lower to higher latitudes along the same magnetic meridian. These onsets are immediately followed by poleward moving signatures that are only observed at higher-latitude stations in the both hemispheres. At lower-latitude stations, these onsets are followed by micropositive bays. We argue that these observational results can be explained by throat auroras being caused by low-latitude magnetopause reconnection.

a. *Concurrent onsets and the followed poleward moving signature*. Based on previous studies (e.g. Southwood, 1987), when a low-latitude reconnection occurs on the dayside magnetopause, a pair of field-aligned currents (FACs) flowing upward and downward will be generated and the geomagnetic variations observed on the ground can be accounted for the effect of two Hall current vortices in the polar ionosphere driven by the FACs. In addition, magnetic reconnection is a burst process for magnetic energy converting into kinetic energy. In response to the first arrival of the burst reconnection signal to the ionosphere, the initial ionospheric responses can be accounted for a sudden increase of an ionospheric electric field, so this effect should be observed simultaneously in all detectable areas. In Figures 4 and 5, as indicated by the vertical lines, we see that the onsets were almost simultaneously observed at all stations from lower to higher latitudes (even in the Southern Hemisphere). We argue that these concurrent onsets reflect the first arrival of the reconnection signal at the ionosphere for two reconnections, which correspond to the throat aurora brightenings as shown in Figures 4 and 5.

As soon as the reconnection signal arrives at the ionosphere, it will create two Hall current vortices centered with the upward and downward FACs that are in anticlockwise and clockwise, respectively, in the Northern Hemisphere (e.g., Southwood, 1987). Correspondent to the anticlockwise Hall current vortex that is centered with the upward FAC, the stations at lower- and higher-latitude sides of the FAC's footprint will observe increases and decreases in the *X* component, respectively. For the concurrent onsets observed at ~09:28:30 UT, we infer that the upward FAC's footprint should be at somewhere close to the latitude of STF or ATU, because the *X* component observed at lower- and higher-latitude sides of STF and ATU show approximate antiphase variation and the variations at STF and ATU seem like in a transition stage. Under such condition, all the concurrent onsets and the antiphase variations observed at higher and lower latitudes after the onsets, as shown in Figures 4 and 5, can be well explained.

After the reconnection signal being detected, the footprint of newly opened field lines will be dragged to move antisunward (poleward) under magnetic tension force. Now we consider the footprint for the upward FAC in the Northern Hemisphere, which is the center of the anticlockwise ionospheric currents vortex. Initially, the *X* component observed at higher-latitude side of the FAC's footprint will show decreases because the ionospheric currents overhead of these station flow westward. As soon as the FAC's footprint moves from low-latitude side to high-latitude side of a station, the *X* component observed at this station will immediately show increase and result in a negative peak in the observation. Therefore, with the upward FAC's footprint moving over the stations from lower to higher latitudes, a poleward moving negative peak can be observed at those stations one by one, just as shown in Figures 4 and 5.

b. *The interhemispheric conjugacy*. Based on the scenario discussed above, the interhemispheric conjugate properties for the higher- and lower-latitude stations should be different. For the lower-latitude stations in the both hemispheres, they are on the closed field lines, so their observations should be much similar. For the higher-latitude stations in the two hemispheres, their observations should separately reflect the poleward dragging of the newly opened field lines and will not necessarily be as similar. We suggest that these expectations are well displayed in Figure 4. We see that the similarity for the observations at conjugate stations at lower latitudes (e.g., SKT/PG4 and GHB/PG5) are much better than those observed at higher latitudes (e.g., UPN/PG0 and UMQ/PG1).

Figure 4 shows that the concurrent onsets and the followed poleward moving signature were also observed in the Southern Hemisphere. We see that the negative peaks observed at conjugate stations show a little time lag between the Southern and Northern Hemispheres. The Northern Hemisphere is slightly leading as indicated by the dashed lines. This may reflect the reconnection site was closer to the northern cusp.

c. *Micropositive bay associated with throat aurora*. It has been well known that substorm current wedge consists of a pair of FACs flowing downward in the east and upward in the west. At a midlatitude station located between the upward and downward FACs near midnight, a positive pulse in the X component can be often observed during a substrom expansion phase, which is called midlatitude positive bay (e.g., Kepko et al., 2014; McPherron et al., 1973). The midlatitude positive bay generally rises for more than 20 min and decays slowly. In Figures 4 and 5, we observed X component increases at the lower-latitude stations after the concurrent onsets with time duration no longer than 10 min, which we call micropositive bay. We suggest that the micropositive bay observed near magnetic local noon is generated by the same mechanism as the midlatitude positive bay observed near midnight, which are both generated by a pair of FACs flowing downward in the east and upward in the west. The difference is that midlatitude positive bays is associated with substorm, while micropositive bay is related with throat aurora.

In Figure 4, multiple north-south aligned throat auroras were simultaneously observed. This means that the FACs associated with these throat auroras may be in multiple sheets, that is, more than a pair of FACs. Under such condition, a station located between a pair of FACs that flow downward in the east and upward in the west will observe a micropositive bay. If a station located between a pair of FACs that flow downward in the west and upward in the east, it will observe decrease in the X component, just like a micronegative bay. This can explain why the variations observed at Norwegian line stations shown antiphase with those observed at Greenland-West stations after the onset at ~09:36:30 UT in Figure 4 and after the onset at ~08:19:00 UT in Figure 5.

d. *Compare with previous studies on geomagnetic transients near local noon*. Geomagnetic transients observed at high latitudes on the dayside have been extensively studied, including, MIE (Lanzerotti et al., 1990), TCV (Chaston et al., 1993; Friis-Christensen et al., 1988; Glassmeier et al., 1989; Shi et al., 2014; Zesta, 2002), and impulsive ULF waves (Kozyreva et al., 2019; Lyatsky & Sibeck, 1997; Olson, 1986; Shen et al., 2018). MIEs have been generally accounted for geomagnetic responses to the transient variations in the IMF or solar wind pressure (Kataoka, 2003; Kawano et al., 1992; Lanzerotti et al., 1990; Lin et al., 1995; Mende et al., 1990; Sibeck & Croley, 1991). TCV can be regarded as a particular type of MIE, which are characterized by a series of vortices representing $E \times B$ convection propagating longitudinally from the dayside to nightside with a duration of a few minutes to half an hour. TCVs were initially observed by ground-based magnetometers and have been considered as the signature of flux transfer event (FTE) (Konik et al., 1994; Lanzerotti et al., 1986). However, because TCV often displays in transient ULF waveforms (Friis-Christensen et al., 1988; Kozyreva et al., 2019; Lyatsky & Sibeck, 1997; Shi et al., 2014) and have conjugated properties (Kim et al., 2015; Murr, 2002), they have been suggested as ground signature of surface waves generated on the closed field lines. It is very difficult to distinguish the differences among the MIEs, TCVs, and impulsive ULF waves, so Zesta (2002) treated all these events as TCVs and classified them into “isolated” and “nonisolated” ones, which are suggested to be correspondent to different source mechanisms.

The auroral responses associated with geomagnetic observations of MIEs (Mende et al., 1990), TCVs (Kim et al., 2017; Murr, 2002), and impulsive ULF waves (Kozyreva et al., 2019) have also been investigated. In these studies, we noticed that all of the auroras had clear throat aurora properties, but they were just treated as transient responses to a sudden changes of the solar wind conditions (Kim et al., 2017; Kozyreva et al., 2019; Mende et al., 2001) and no attention had been paid to what particular magnetospheric processes can be reflected by these particular auroral forms. Compared with these previous studies, this paper reported some new information as follows.

First, we stress that throat aurora refers to a particular north-south aligned discrete auroral form that is extending from the equatorward edge of the discrete auroral oval but is not intensification of an auroral structure that is inside the original aurora oval. Throat aurora has been suggested to correspond to a magnetopause indentation that is caused by magnetopause reconnection (Han et al., 2019). We found that all the auroras shown in Kim et al. (2017), Kozyreva et al. (2019), and Mende et al. (2001) have clear throat aurora features. We argue that the geomagnetic responses discussed in these studies should correspond to localized magnetopause indentations that are caused by magnetopause reconnection. The surface waves observed in Kozyreva et al. (2019) and the traveling properties observed in Kim et al. (2017) should be the resultant effects observed at lower- and higher-latitude sides of the newly opened field lines, respectively.

Second, we show that throat aurora and the associated geomagnetic transients can also be observed under stable and quiet solar wind conditions but are unnecessarily correspondent with sudden changes of IMF or solar wind conditions (hereafter call them "discontinuities") as discussed in previous studies (Kim et al., 2017; Kozyreva et al., 2019; Mende et al., 2001). This can be explained based on previous studies on throat aurora. Statistical study (Han et al., 2017) suggested that occurrence of throat aurora should be affected by the magnetosheath high-speed jet (HSJ), while the HSJ prefer to be observed under stable and quiet solar wind conditions (Plaschke et al., 2013, 2018). This means that the transient processes locally generated in the magnetosheath (e.g., HSJ) under quiet and stable solar wind conditions can also cause clear geomagnetic and auroral responses that are similar with those caused by discontinuities (e.g., Kim et al., 2017; Kozyreva et al., 2019; Mende et al., 2001).

We believe that the previous studies (e.g., Kim et al., 2017; Kozyreva et al., 2019; Mende et al., 2001) have shown throat auroras being observed in respond to discontinuities. This has important implications. The spatial scale of magnetopause indentation as inferred from the observation of throat aurora is no more than ~3 Re (Earth Radius) in east-west extension (Zhou et al., 2020), while the spatial scale of discontinuity observed in OMNI data is generally larger than ~3 Re. This discrepancy in spatial scale implies that the discontinuities should not cause throat auroras by directly interacting with the magnetopause, but by first producing HSJs in the magnetosheath and then the HSJs interacting with magnetopause and producing the throat auroras. This is consistent with some previous studies on HSJ, which suggested that HSJs can be generated in response to discontinuities (Archer et al., 2012; Dmitriev & Suvorova, 2015).

e. *Implications on the magnetic transients observed near local noon*. Geomagnetic transients observed near magnetic local noon at high latitude include TCVs, MIEs, and impulsive ULF waves. In Figure 4, associated with two successive throat auroras, we identified two concurrent onsets that were both followed by poleward moving signatures and micropositive bays observed at the higher- and lower-latitude stations, respectively. The poleward moving signature observed at higher-latitude stations may be identified as TCVs. The successive micropositive bays observed at lower-latitude stations may be treated as impulsive ULF wave. Therefore, we suggest that some of the geomagnetic transients observed at high latitudes near local noon may be analyzed by the same method as used in this study to investigate whether or not they are correspondent with magnetopause reconnection. The method is to identify a concurrent onset from the X component along a meridian first and then to check if there are a poleward moving negative peak and micropositive bays observed at higher- and lower-latitude stations, respectively.

5. Conclusions

In order to investigate the conjugacy of throat aurora, we examined the geomagnetic variations associated with throat aurora observed from conjugate stations from the Northern and Southern Hemispheres. We found that throat aurora and clear geomagnetic responses can be observed under quiet and stable solar wind conditions. This may reflect that transient processes, such as HSJ, locally generated in the magnetosheath under quiet solar wind condition can cause indentations on the magnetopause, as well as result in throat aurora and geomagnetic responses on the ground. In the geomagnetic observations, we identified concurrent onsets at all of the stations along the same meridian associated with the brightening of throat aurora. Immediately after the concurrent onsets, we observed poleward moving signature at higher-latitude stations and micropositive bays at lower-latitude stations. We suggest that these are evidence for throat aurora being caused by magnetopause (low-latitude) reconnection. We suggest that the concurrent onsets reflect the first arrival of the reconnection signal at the ionosphere, that the poleward moving signature reflect newly opened field lines dragging antisunward, and that the micropositive bays are caused by a pair of FACs that are generated during the reconnection. This may provide a new method for analyzing the geomagnetic transients observed at high latitude near magnetic local noon.

Data Availability Statement

Magnetometer data from the Greenland Magnetometer Array were provided by the National Space Institute at the Technical University of Denmark (DTU Space) (http://flux.phys.uit.no/ascii/); magnetometer data from Norwegian magnetometers were provided by the Tromsø Geophysical Observatory (TGO) (http://flux.phys.uit.no/geomag.html).

Acknowledgments
This work was supported by the National Natural Science Foundation of China 41774174, 41974185, and 41831072. We acknowledge use of NASA/GSFC's Space Physics Data Facility's OMNIWeb service (at https://cdaweb.gsfc.nasa.gov/index.html/). We acknowledge the auroral observations at YRS supported from Chinese National Antarctic & Arctic Data Centre (CN-NADC), National Earth System Science Data Sharing Infrastructure, National Science & Technology Infrastructure of China, which are provided by The Polar Atmospheric and Space Physics Research Division (PASP) at Polar Research Institute of China through http://www.chinare.org.cn/uap/database. The Antarctic AAL-PIP data have been provided by Virginia Tech, which is supported by the National Science Foundation through the following awards for this purpose: ANT0839858, ATM922979, ANT0838861, PLR-1243398, and PLR-1543364 (http://mist.nianet.org/).

References

Archer, M. O., Horbury, T. S., & Eastwood, J. P. (2012). Magnetosheath pressure pulses: Generation downstream of the bow shock from solar wind discontinuities. *Journal of Geophysical Research*, *117*, 05228. https://doi.org/10.1029/2011JA017468

Chaston, C. C., Hansen, H. J., Menk, F. W., Fraser, B. J., & Hu, Y. D. (1993). Ground signatures of convecting reconnected flux tubes. *Journal of Geophysical Research*, *98*(A11), 19,151–19,161. https://doi.org/10.1029/93ja00739

Chen, X. C., Han, D. S., Lorentzen, D. A., Oksavik, K., Moen, J. I., & Baddeley, L. J. (2017). Dynamic properties of throat aurora revealed by simultaneous ground and satellite observations. *Journal of Geophysical Research: Space Physics*, *122*, 3469–3486. https://doi.org/10.1002/2016JA023033

Dmitriev, A. V., & Suvorova, A. V. (2015). Large-scale jets in the magnetosheath and plasma penetration across the magnetopause: THEMIS observations. *Journal of Geophysical Research: Space Physics*, *120*, 4423–4437. https://doi.org/10.1002/2014JA020953

Friis-Christensen, E., McHenry, M. A., Clauer, C. R., & Vennerstr?m, S. (1988). Ionospheric traveling convection vortices observed near the polar cleft: A triggered response to sudden changes in the solar wind. *Geophysical Research Letters*, *15*(3), 253–256. https://doi.org/10.1029/GL015i003p00253

Glassmeier, K.-H., Hönisch, M., & Untiedt, J. (1989). Ground-based and satellite observations of traveling magnetospheric convection twin vortices. *Journal of Geophysical Research*, *94*(A3), 2520–2528. https://doi.org/10.1029/JA094iA03p02520

Han, D. (2019). Ionospheric polarization electric field guiding magnetopause reconnection: A conceptual model of throat aurora. *Science China Earth Sciences*, *62*(12), 2099–2105. https://doi.org/10.1007/s11430-019-9358-8

Han, D., Chen, X.-C., Liu, J.-J., Qiu, Q., Keika, K., Hu, Z.-J., et al. (2015). An extensive survey of dayside diffuse aurora based on optical observations at Yellow River Station. *Journal of Geophysical Research: Space Physics*, *120*, 7447–7465. https://doi.org/10.1002/2015ja021699

Han, D. S., Hietala, H., Chen, X. C., Nishimura, Y., Lyons, L. R., Liu, J. J., et al. (2017). Observational properties of dayside throat aurora and implications on the possible generation mechanisms. *Journal of Geophysical Research: Space Physics*, *122*, 1853–1870. https://doi.org/10.1002/2016ja023394

Han, D. S., Liu, J. J., Chen, X. C., Xu, T., Li, B., Hu, Z. J., et al. (2018). Direct evidence for throat aurora being the ionospheric signature of magnetopause transient and reflecting localized magnetopause indentations. *Journal of Geophysical Research: Space Physics*, *123*, 2658–2667. https://doi.org/10.1002/2017JA024945

Han, D.-S., Nishimura, Y., Lyons, L. R., Hu, H. Q., & Yang, H. G. (2016). Throat aurora: The ionospheric signature of magnetosheath particles penetrating into the magnetosphere. *Geophysical Research Letters*, *43*, 1819–1827. https://doi.org/10.1002/2016gl068181

Han, D.-S., Xu, T., Jin, Y., Oksavik, K., Chen, X.-C., Liu, J.-J., et al. (2019). Observational evidence for throat aurora being associated with magnetopause reconnection. *Geophysical Research Letters*, *46*, 7113–7120. https://doi.org/10.1029/2019GL083593

Kataoka, R. (2003). Statistical identification of solar wind origins of magnetic impulse events. *Journal of Geophysical Research*, *108*(A12), 1436. https://doi.org/10.1029/2003ja010202

Kawano, H., Kokubun, S., & Takahashi, K. (1992). Survey of transient magnetic field events in the dayside magnetosphere. *Journal of Geophysical Research*, *97*(A7), 10,677–10,692. https://doi.org/10.1029/92ja00369

Kepko, L., McPherron, R. L., Amm, O., Apatenkov, S., Baumjohann, W., Birn, J., et al. (2014). Substorm current wedge revisited. *Space Science Reviews*, *190*(1–4), 1–46. https://doi.org/10.1007/s11214-014-0124-9

Kim, H., Clauer, C. R., Engebretson, M. J., Matzka, J., Sibeck, D. G., Singer, H. J., et al. (2015). Conjugate observations of traveling convection vortices associated with transient events at the magnetopause. *Journal of Geophysical Research: Space Physics*, *120*, 2015–2035. https://doi.org/10.1002/2014ja020743

Kim, H., Lessard, M. R., Jones, S. L., Lynch, K. A., Fernandes, P. A., Aruliah, A. L., et al. (2017). Simultaneous observations of traveling convection vortices: Ionosphere-thermosphere coupling. *Journal of Geophysical Research: Space Physics*, *122*, 4943–4959. https://doi.org/10.1002/2017ja023904

Konik, R. M., Lanzerotti, L. J., Wolfe, A., Maclennan, C. G., & Venkatesan, D. (1994). Cusp latitude magnetic impulse events: 2. Interplanetary magnetic field and solar wind conditions. *Journal of Geophysical Research*, *99*(A8), 14,831–14,853. https://doi.org/10.1029/93ja03241

Kozyreva, O., Pilipenko, V., Lorentzen, D., Baddeley, L., & Hartinger, M. (2019). Transient oscillations near the dayside open-closed boundary: Evidence of magnetopause surface mode? *Journal of Geophysical Research: Space Physics*, *124*, 9058–9074. https://doi.org/10.1029/2018ja025684

Lanzerotti, L. J., Lee, L. C., Maclennan, C. G., Wolfe, A., & Medford, L. V. (1986). Possible evidence of flux transfer events in the polar ionosphere. *Geophysical Research Letters*, *13*(11), 1089–1092. https://doi.org/10.1029/GL013i011p01089

Lanzerotti, L. J., Wolfe, A., Trivedi, N., Maclennan, C. G., & Medford, L. V. (1990). Magnetic impulse events at high latitudes: Magnetopause and boundary layer plasma processes. *Journal of Geophysical Research*, *95*(A1), 97–107. https://doi.org/10.1029/JA095iA01p00097

Lin, Z. M., Bering, E. A., Benbrook, J. R., Liao, B., Lanzerotti, L. J., Maclennan, C. G., et al. (1995). Statistical studies of impulsive events at high latitudes. *Journal of Geophysical Research*, *100*(A5), 7553–7566. https://doi.org/10.1029/94ja01655

Lockwood, M. (1997). Relationship of dayside auroral precipitations to the open-closed separatrix and the pattern of convective flow. *Journal of Geophysical Research*, *102*(A8), 17,475–17,487. https://doi.org/10.1029/97JA01100

Lyatsky, W. B., & Sibeck, D. G. (1997). Surface waves on the low-latitude boundary layer inner edge and travelling convection vortices. *Journal of Geophysical Research*, *102*(A8), 17,643–17,647. https://doi.org/10.1029/97ja00323

McPherron, R. L., Russell, C. T., & Aubry, M. P. (1973). Satellite studies of magnetospheric substorms on August 15.1968. 9. Phenomenological model for substorms. *Journal of Geophysical Research*, *78*(16), 3131–3149. https://doi.org/10.1029/JA078i016p03131

Mende, S. B., Frey, H. U., Doolittle, J. H., Lanzerotti, L., & Maclennan, C. G. (2001). Dayside optical and magnetic correlation events. *Journal of Geophysical Research*, *106*(A11), 24,637–24,649. https://doi.org/10.1029/2001ja900065

Mende, S. B., Rairden, R. L., Lanzerotti, L. J., & Maclennan, C. G. (1990). Magnetic impulses and associated optical signatures in the dayside aurora. *Geophysical Research Letters*, *17*(2), 131–134. https://doi.org/10.1029/GL017i002p00131

Moen, J., Evans, D., Carlson, H. C., & Lockwood, M. (1996). Dayside moving auroral transients related to LLBL dynamics. *Geophysical Research Letters*, *23*(22), 3247–3250. https://doi.org/10.1029/96gl02766

Murr, D. L. (2002). Conjugate observations of traveling convection vortices: The field-aligned current system. *Journal of Geophysical Research*, *107*(A10), 1306. https://doi.org/10.1029/2002ja009456

Olson, J. V. (1986). ULF signatures of the polar cusp. *Journal of Geophysical Research*, *91*(A9), 10,055–10,062. https://doi.org/10.1029/JA091iA09p10055

Plaschke, F., Hietala, H., & Angelopoulos, V. (2013). Anti-sunward high-speed jets in the subsolar magnetosheath. *Annales Geophysicae*, *31*(10), 1877–1889. https://doi.org/10.5194/angeo-31-1877-2013

Plaschke, F., Hietala, H., Archer, M., Blanco-Cano, X., Kajdič, P., Karlsson, T., et al. (2018). Jets downstream of collisionless shocks. *Space Science Reviews*, *214*, 81. https://doi.org/10.1007/s11214-018-0516-3

Sandholt, P. E., & Newell, P. T. (1992). Ground and satellite obervations of an auroral event at the cusp/cleft equatorward boundary. *Journal of Geophysical Research*, *97*(A6), 8685–8691. https://doi.org/10.1029/91JA02995

Shen, X.-C., Shi, Q., Wang, B., Zhang, H., Hudson, M. K., Nishimura, Y., et al. (2018). Dayside magnetospheric and ionospheric responses to a foreshock transient on 25 June 2008: 1. FLR observed by satellite and ground-based magnetometers. *Journal of Geophysical Research: Space Physics*, *123*, 6335–6346. https://doi.org/10.1029/2018ja025349

Shi, Q. Q., Hartinger, M. D., Angelopoulos, V., Tian, A. M., Fu, S. Y., Zong, Q. G., et al. (2014). Solar wind pressure pulse-driven magnetospheric vortices and their global consequences. *Journal of Geophysical Research: Space Physics*, *119*, 4274–4280. https://doi.org/10.1002/2013ja019551

Sibeck, D. G., & Croley, D. J. (1991). Solar wind dynamic pressure variations and possible ground signatures of flux transfer events. *Journal of Geophysical Research*, *96*(A2), 1669–1683. https://doi.org/10.1029/90ja02357

Southwood, D. J. (1987). The ionospheric signature of flux transfer events. *Journal of Geophysical Research*, *92*(A4), 3207–3213. https://doi.org/10.1029/JA092iA04p03207

Xu, Z. H., Hartinger, M. D., Clauer, R., Weimer, D., Deshpande, K., Kim, H., et al. (2019). Newly established autonomous adaptive low-power instrument platform (AAL-PIP) chain on East Antarctic Plateau and operation. *Advances in Polar Science*, *30*(4), 362–374. https://doi.org/10.13679/j.advps.2019.0028

Zesta, E. (2002). A statistical study of traveling convection vortices using the Magnetometer Array for Cusp and Cleft Studies. *Journal of Geophysical Research*, *107*(A10), 1317. https://doi.org/10.1029/1999ja000386

Zhou, S., Han, D., Gokani, S. A., Selvakumaran, R., & Zhang, Y. (2020). Throat aurora observed by DMSP/SSUSI in a global view. *Science China Earth Sciences*, *63*, 891–898. https://doi.org/10.1007/s11430-019-9592-y